

# Operando systems for the evaluation of the catalytic performance of NO<sub>x</sub> storage and reduction materials

B.I. Mosqueda-Jiménez<sup>a,d,\*</sup>, A. Lahougue<sup>a</sup>, P. Bazin<sup>a</sup>, V. Harlé<sup>b</sup>,  
G. Blanchard<sup>b</sup>, A. Sassi<sup>c</sup>, M. Daturi<sup>a</sup>

<sup>a</sup> *Laboratoire Catalyse et Spectrochimie, UMR 6506, ENSICAen 6, bd Maréchal Juin, 14050 Caen Cedex, France*

<sup>b</sup> *Rhodia Recherches, 52 Rue de la Haie Coq, 93308 Aubervilliers Cedex, France*

<sup>c</sup> *Peugeot Citroën Automobiles, 18 Rue des Fauvelles, 92256 La Garenne-Colombes, France*

<sup>d</sup> *Laboratoire d'Application de la Chimie à l'Environnement, CNRS UMR 5634,  
43 bd du 11 novembre 1918, 69622 Villeurbanne, France*

Available online 18 September 2006

## Abstract

Operando measurements were carried out in a quartz reactor to evaluate the catalytic performance of NO<sub>x</sub> storage and reduction materials containing Pt and Ba supported on Al<sub>2</sub>O<sub>3</sub>. Carbonates present on the surface after activation were removed after the first exposure of the sample to the nitration flow. Nitrite species bound to barium were observed at low temperatures. Barium nitrates are the predominant species in the studied temperature range under wet and dry conditions. These species are not stable at temperatures above 723 K. The presence of water inhibits the formation of alumina nitrates favoring the coordination of nitrates with the barium sites.

© 2006 Elsevier B.V. All rights reserved.

**Keywords:** Operando; NO<sub>x</sub>; Nitration; Activation

## 1. Introduction

In the search of more energetically and ecologically efficient systems, NO<sub>x</sub> storage and reduction catalysts represent one alternative for the emission control from automotive sources [1–4]. These catalysts are predominantly used for the exhaust control of lean-burn engines resulting in lower overall CO<sub>2</sub> emissions. The lowering of NO<sub>x</sub> emissions using this type of technology leads to the increase of fuel consumption (catalyst management) and high after treatment price (precious metal loading). Knowing that this technology is still under development, the actual commercially available technologies do not allow meeting the NO<sub>x</sub> reduction targets after high mileage.

Optimization of this technology in terms of durability and definition of the best trade off between fuel consumption (CO<sub>2</sub> emissions) induced by catalyst management, price and NO<sub>x</sub>

reduction is needed for an extended and efficient serial application. Deep understanding of the chemical mechanisms taking place on this catalyst in real working conditions is needed to reach the above-mentioned goals.

Due to the complexity of commercial NO<sub>x</sub> trap impregnations, high precision “operando” analytical tools adapted to this technology can help understanding the catalyst behavior under simulated representative gas and temperature conditions.

The aim of the present work was to study the phenomena occurring on a Pt/Ba/CeO<sub>2</sub>–ZrO<sub>2</sub>/Al<sub>2</sub>O<sub>3</sub> catalyst during the NO<sub>x</sub> storage by using a newly designed cell that allows time-resolved measurements under flow at temperatures as high as 873 K.

## 2. Experimental

### 2.1. Materials

The commercial NO<sub>x</sub> storage catalyst was supplied by Rhodia. The material contains Pt, Ba, CeO<sub>2</sub>, ZrO<sub>2</sub> supported on Al<sub>2</sub>O<sub>3</sub>. Prior to any study, the catalyst was aged at 1123 K using a mixture of air and water (10 vol.%) during 12 h.

\* Corresponding author.

E-mail address: [Bertha.Mosqueda@univ-lyon1.fr](mailto:Bertha.Mosqueda@univ-lyon1.fr)

(B.I. Mosqueda-Jiménez).

## 2.2. Operando measurements

The material was pressed into self-supporting wafers of  $10 \text{ mg cm}^{-2}$  and placed into the quartz reactor equipped with KBr windows. For the analysis of the surface, operando measurements were carried out with a Nicolet FT-IR Nexus spectrometer equipped with a MCT detector. FT-IR spectra were collected with a resolution of  $4 \text{ cm}^{-1}$ . The analysis of the outlet gases was performed by means of a Pfeiffer Omnistar mass spectrometer. Likewise FT-IR spectra of the gas phase were collected using a gas microcell.

The sample was activated *in situ* by heating from room temperature to 873 K over 3 h under a flow of 10% oxygen in argon. Then the temperature was decreased to the nitration temperature. Different temperatures ranging from 473 to 873 K were tested. Experiments were performed at a total flow of  $25 \text{ cm}^3 \text{ min}^{-1}$ . Concentrations of the reactants were 500 ppm NO, 10% oxygen, and 1.5% water. Argon was used as the carrier gas.

The exposure of the sample to the nitration flow was carried out during 120 min. Weakly adsorbed surface species were desorbed by flushing the cell with a flow of 1.5% water in argon during 30 min at the nitration temperature. The desorption of the strongly adsorbed surface species was carried out by increasing the temperature with an increment of  $5 \text{ K min}^{-1}$  until 873 K under a flow of 1.5% water in argon.

## 3. Results and discussion

### 3.1. Activation

Intense bands at  $1467$  and  $1434 \text{ cm}^{-1}$  attributed to polydentate carbonates [5–7] were observed before the activation of the sample. Pairs of bands at  $1536$  and  $1371 \text{ cm}^{-1}$ ,  $1506$  and  $1400 \text{ cm}^{-1}$  corresponding to the  $\nu_3$  and  $\nu_3''$  vibrations of two different types of monodentate and polydentate carbonates (average  $\sim 1450 \text{ cm}^{-1}$ ) were detected as well. After the pretreatment in oxygen at 873 K, these species were still observed but the intensities of the corresponding bands were much weaker.

### 3.2. Nitration

#### 3.2.1. On the carbonated surface

The activated sample was exposed to the wet nitration flow at 623 K. In order to facilitate the bands attribution, the difference spectra obtained by subtraction of the spectra collected during nitration are shown in Fig. 1. The formation of polydentate nitrates on barium occurring mainly during the first 30 min of the nitration was observed by the presence of the bands at  $1415$  and  $1328 \text{ cm}^{-1}$  [8,9]. Other nitrates, most probably monodentate nitrates, associated to the bands at  $1472$  and  $1272 \text{ cm}^{-1}$  were detected at earlier times. Additional nitrate species adsorbed at the interface between  $\text{Al}^{3+}$  and  $\text{Ba}^{2+}$  were observed by the presence of the bands at  $1544$  and  $1226 \text{ cm}^{-1}$  [8]. The band at  $1028 \text{ cm}^{-1}$  results from the  $\nu_1$  vibrational mode of the nitrate species [10]. The bands at  $1351$  and  $1387 \text{ cm}^{-1}$  observed during the last minutes of the nitration and increasing with time are attributed to ionic nitrates formed on the KBr [11] windows

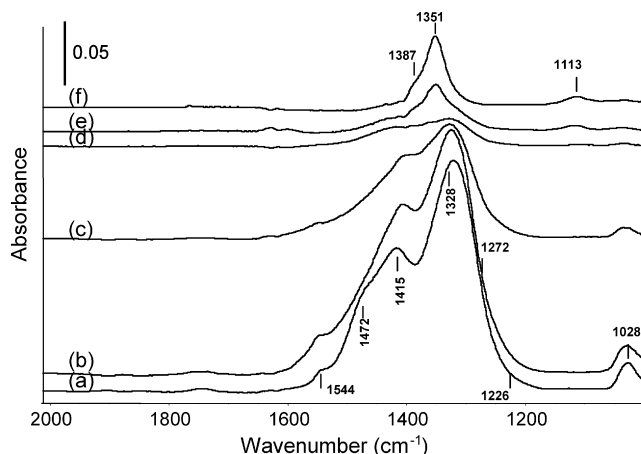


Fig. 1. Difference spectra of the surface collected during the nitration of the sample (carbonated surface) at 623 K. (a) 5–1 min; (b) 10–5 min; (c) 20–10 min; (d) 30–20 min; (e) 60–30 min; (f) 120–60 min.

(spectra e and f, Fig. 1). The temperature programmed desorption carried out after the nitration caused the complete desorption of the nitrate species, recovering an infrared spectrum similar to that obtained after the activation with oxygen, except for the carbonate bands which were no longer present.

#### 3.2.2. In the presence of water—effect of temperature

Wet nitration was carried out between 473 and 873 K. Fig. 2A shows the evolution of the surface species with time for the first 5 min of the nitration at 473 K. Bands at  $1214$ ,  $1152$ ,  $1414$  and  $1328 \text{ cm}^{-1}$  were observed during the first moments of exposure of the sample to the nitration flow. The  $1214$  and  $1152 \text{ cm}^{-1}$  bands can be assigned to nitrite species bound to barium [12–16]. The weak bands at  $1414$  and  $1328 \text{ cm}^{-1}$  are assigned to the  $\nu_3$  and  $\nu_3''$  vibrations of surface nitrate species [15]. As a function of time the rate of formation of the nitrite species decreased and that of the nitrate species increased. In the difference spectrum at 5 min (spectrum h in Fig. 2A) another nitrate species was observed by the presence of the band at  $1470 \text{ cm}^{-1}$ . Its coupled vibration is most likely masked in the broad band observed in the  $1500$ – $1000 \text{ cm}^{-1}$  range. The difference spectra of the nitration until 120 min are shown in Fig. 2B. Nitrite species started to disappear after 20 min of adsorption. At the end of the 120-min nitration, species with bands at  $1426$  and  $1331 \text{ cm}^{-1}$ ,  $1453$  and  $1302 \text{ cm}^{-1}$ ,  $1482$  and  $1269 \text{ cm}^{-1}$ , as well as  $1516$  and  $1243 \text{ cm}^{-1}$  were the most abundant species on the surface. These bands are attributed to the splitting of the  $\nu_3$  vibration of surface nitrates coordinated to energetically-different barium sites [13,17]. We can observe, by looking at the evolution of the bands, that after 120 min of exposure of the sample to the nitration flow the surface was still not saturated.

The formation of nitrites was not very clear during the first moments of the nitration at 623 K [18]. Three different nitrate species associated to the pairs of bands at  $1473$  and  $1273 \text{ cm}^{-1}$ ,  $1437$  and  $1300 \text{ cm}^{-1}$ ,  $1412$  and  $1326 \text{ cm}^{-1}$  were visible (spectrum d in Fig. 3A). Nitrate species bound to the alumina phase were detected by the presence of the band at  $1545 \text{ cm}^{-1}$ , which might be coupled to the band at  $1223 \text{ cm}^{-1}$ . The concentration of nitrate species on barium increased with time.

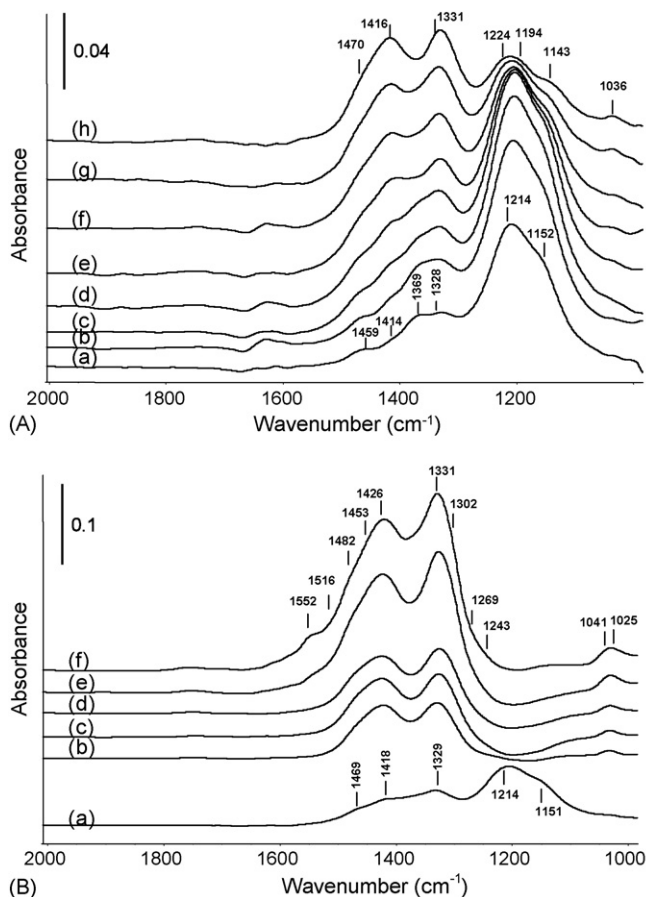


Fig. 2. Difference spectra of the surface collected during the nitration of the sample at 473 K. (A) During the first 5 min: (a) 1.5–1 min; (b) 2–1.5 min; (c) 2.5–2 min; (d) 3–2.5 min; (e) 3.5–3 min; (f) 4–3.5 min; (g) 4.5–4 min; (h) 5–4.5 min. (B) During the 120-min nitration period: (a) 5–1 min; (b) 10–5 min; (c) 20–10 min; (d) 30–20 min; (e) 60–30 min; (f) 120–60 min.

During the nitration in the presence of water at 873 K, similar bands to those observed at 623 K were visible. However, at 873 K the nitrate species bound to barium were formed only during the first 10 min and they were present in very small amounts as indicated by the intensity of the infrared bands (spectrum i in Fig. 3A).

### 3.2.3. Desorption

Desorption at 473 K under a flow of 1.5% water in argon, carried out after the nitration, shows that the nitrate species were stable at 473 K. Desorption of the nitrate species began as soon as the temperature started increasing, and they were not present any longer at temperatures above 773 K.

Surface nitrates formed at 623 K were adsorbed weakly and disappeared during the desorption at constant temperature. The desorption speed increased when the temperature started increasing and they were completely removed when reaching 723 K. Consequently, after the nitration at 873 K, all the surface species disappeared during the first moments of the desorption at 873 K under the flow of 1.5% water in argon.

Similar barium nitrate species were formed during the nitration of the sample in the temperature range between 473 and 873 K. However, stabilities of these species were

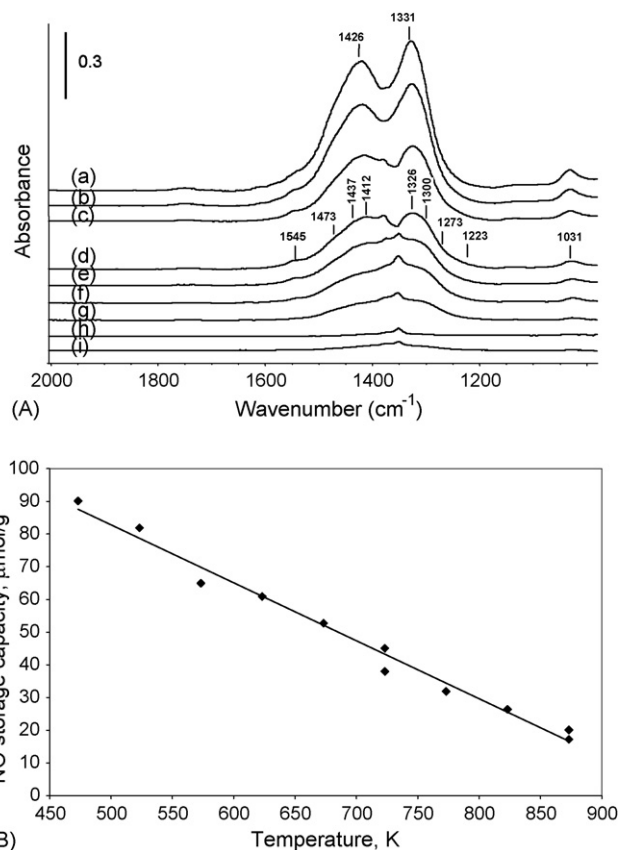


Fig. 3. (A) Surface spectra after 120-min nitration at (a) 473 K; (b) 523 K; (c) 573 K; (d) 623 K; (e) 673 K; (f) 723 K; (g) 773 K; (h) 823 K; (i) 873 K. (B) Variation with temperature of the NO<sub>x</sub> storage capacity calculated for the 120-min nitration.

different, which may suggest that they are coordinated to several types of barium sites [19–21], having different basicity and therefore they are able to stabilize nitrates at different temperatures.

### 3.2.4. Nitration in the absence of water

The water effect was studied by exposing the sample to the nitration flow in the absence of water. Fig. 4A shows the infrared spectra resulting from the nitration of the material under dry conditions at 573 K. In contrast to the wet nitration, for the nitration in the absence of water two intense bands at 1554 and 1245  $\text{cm}^{-1}$  were visible. These bands have been attributed to the  $\nu_3$  split mode of surface nitrates interacting with alumina [11,13,22]. Bands at 1480 and 1257  $\text{cm}^{-1}$ , 1444 and 1299  $\text{cm}^{-1}$ , 1417 and 1331  $\text{cm}^{-1}$  resulted from the presence of nitrate species on barium coexisting on the surface.

To confirm that the formation of nitrates on alumina was the result of the absence of water during the nitration, water was introduced into the system once that the wafer had been exposed to the dry nitration flow. The spectra resulting from this experiment are shown in Fig. 4B. It is clearly observed that adding water to the flow caused the weakening of the bands at 1554 and 1245  $\text{cm}^{-1}$  and the increase of the intensity of the bands at 1417 and 1331  $\text{cm}^{-1}$ , indicating the migration of nitrate species from the alumina support to the barium sites.

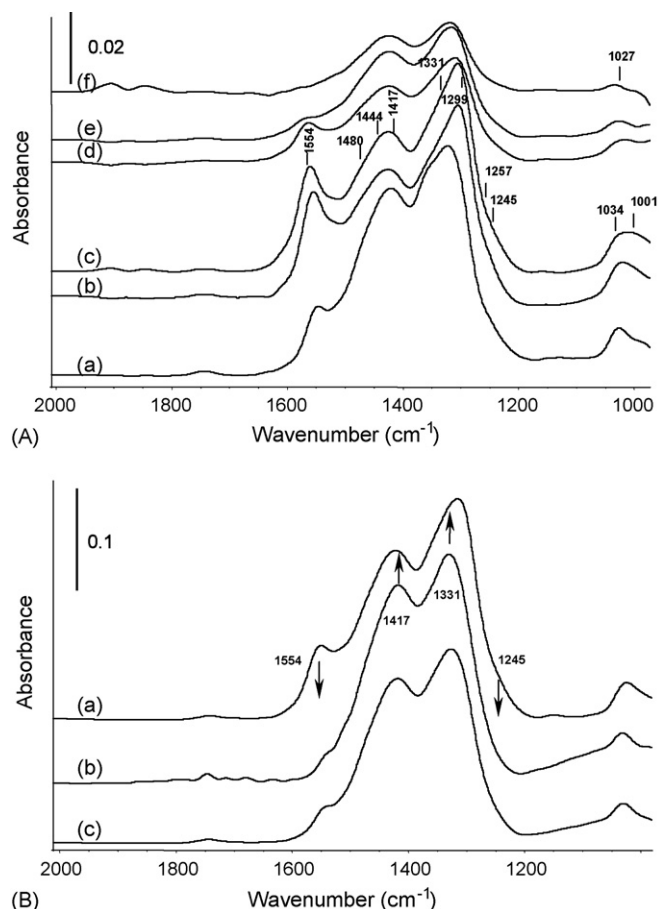


Fig. 4. (A) Difference spectra of the surface during nitration in the absence of water of the sample at 573 K: (a) 5–1 min; (b) 10–5 min; (c) 20–10 min; (d) 30–20 min; (e) 60–30 min; (f) 120–60 min. (B) Infrared spectra collected: (a) after 120 min under the dry nitration flow; (b) under 1.5% water flow; (c) under argon flow.

During the temperature programmed desorption after the dry nitration, it was observed that (similarly to the species formed during the wet nitration [23]) surface nitrates originated from the exposure of the sample to the dry nitration flow were stable up to 723 K. In addition, nitrates bound to alumina desorbed almost completely at 693 K and therefore they were slightly less stable than those on barium.

The rather acid or slightly basic nature of the alumina adsorption sites may cause their preferential interaction with water during the nitration under wet conditions [21], favoring the coordination of the nitrate species with the barium sites.

### 3.2.5. Storage capacity

For each temperature, the amount of  $\text{NO}_x$  stored was calculated from the mass spectrometer data by the difference between the inlet  $\text{NO}_x$  level and the measured  $m/e$  30 signal. The result was verified by the same analysis performed via IR gas spectra. Fig. 3B shows the  $\text{NO}_x$  storage capacity of the material after 120 min of wet nitration, as a function of temperature. Storage capacity decreased with temperature. Thus a maximum of 90  $\mu\text{mol/g}$  was obtained for the nitration at 473 K and a minimum of 17  $\mu\text{mol/g}$  at 873 K. This behavior was attributed to the large dead volume of the reactor, which favors the presence of

$\text{NO}_2$  in the feed gas, which is the rate-determining step for the formation of nitrates [24,25]. In the case of the nitration at 573 K, the storage capacity was higher in the presence of water, compared to that obtained under dry conditions. This indicates that water inhibits the adsorption of nitrates on the alumina support sites allowing their coordination with the barium sites, which have a higher storage capacity and stability.

## 4. Conclusion

Nature, thermal stability and relative amounts of the surface species formed on a commercial catalyst upon NO and  $\text{O}_2$  adsorption in the presence and in the absence of water were analyzed using a novel system consisting of a quartz infrared reactor. Operando measurements showed that carbonates present in the fresh catalyst are removed by replacement with barium nitrate species after the first nitration of the material. Nitrate species coordinated to different barium sites are the predominant surface species under dry and wet conditions. Stabilities of these species are different, suggesting that barium sites possess different basicity and therefore that they are able to stabilize nitrates at different temperatures. At temperatures below 523 K, nitrite species were observed. The presence of water at mild temperatures in the reactant flow makes unavailable for  $\text{NO}_x$  adsorption the alumina adsorption sites. The results obtained in this study can give valuable information about the behavior of typical  $\text{NO}_x$  storage materials in real application conditions.

## Acknowledgements

The authors thank PSA and Rhodia for the award of the postdoctoral fellowship to B.I.M.J.

## References

- [1] W.S. Epling, L.E. Campbell, A. Yezerets, N.W. Currier, J.E. Parks, *Catal. Rev.* 46 (2004) 163.
- [2] S.-I. Matsumoto, *Catal. Today* 90 (2004) 183.
- [3] T. Kanazawa, *Catal. Today* 96 (2004) 171.
- [4] N. Takahashi, H. Shinjoh, T. Iijima, T. Suzuki, K. Yamazaki, K. Yokota, H. Suzuki, N. Miyoshi, S.-I. Matsumoto, T. Tanizawa, *Catal. Today* 27 (1996) 63.
- [5] J.C. Lavalley, *Catal. Today* 27 (1996) 377.
- [6] G. Busca, V. Lorenzelli, *Mater. Chem.* 7 (1982) 89.
- [7] E. Fridell, M. Skoglundh, B. Westerberg, S. Johansson, G. Smedler, *J. Catal.* 183 (1999) 196.
- [8] T. Lesage, C. Verrier, P. Bazin, J. Saussey, M. Daturi, *Phys. Chem. Chem. Phys.* 5 (2003) 4435.
- [9] V.G. Milt, M.A. Ulla, E.E. Miro, *Appl. Catal. B* 57 (2005) 13.
- [10] P.T. Fanson, M.R. Horton, W.N. Delgass, J. Lauterbach, *Appl. Catal. B* 46 (2003) 393.
- [11] T.J. Toops, D.B. Smith, W.P. Partridge, *Appl. Catal. B* 58 (2005) 145.
- [12] H. Mahzoul, J.F. Brilhac, P. Gilot, *Appl. Catal. B* 20 (1999) 47.
- [13] K. Hadjiivanov, *Catal. Rev. Sci. Eng.* 42 (2000) 71.
- [14] L.F. Liotta, A. Macaluso, G.E. Arena, M. Livi, G. Centi, G. Deganello, *Catal. Today* 75 (2002) 439.
- [15] I. Nova, L. Castoldi, L. Lietti, E. Tronconi, P. Forzatti, F. Prinetto, G. Ghiotti, *J. Catal.* 222 (2004) 377.
- [16] Y. Su, M.D. Amiridis, *Catal. Today* 96 (2004) 31.
- [17] Z. Liu, J.A. Anderson, *J. Catal.* 224 (2004) 18.

- [18] F. Prinetto, G. Ghiotti, I. Nova, L. Lietti, E. Tronconi, P. Forzatti, *J. Phys. Chem. B* 105 (2001) 12732.
- [19] M. Piacentini, M. Maciejewski, A. Baiker, *Appl. Catal. B* 59 (2005) 187.
- [20] W.S. Epling, G.C. Campbell, J.E. Parks, *Catal. Lett.* 90 (2003) 45.
- [21] W.S. Epling, J.E. Parks, G.C. Campbell, A. Yezerets, N.W. Currier, L.E. Campbell, *Catal. Today* 96 (2004) 21.
- [22] T.J. Toops, D.B. Smith, W.S. Epling, J.E. Parks, W.P. Partridge, *Appl. Catal. B* 58 (2005) 255.
- [23] N.W. Cant, M.J. Patterson, *Catal. Lett.* 85 (2003) 153.
- [24] C. Hess, J.H. Lunsford, *J. Phys. Chem. B* 106 (2002) 6358.
- [25] P. Broqvist, I. Panas, E. Fridell, H. Persson, *J. Phys. Chem. B* 106 (2002) 137.